Wavelet Spectrum Analysis and Ocean Wind Waves

Paul C. Liu

Abstract. Wavelet spectrum analysis is applied to a set of measured ocean wind waves data collected during the 1990 SWADE (Surface Wave Dynamics Experiment) program. The results reveal significantly new and previously unexplored insights on wave grouping parameterizations, phase relations during wind wave growth, and detecting wave breaking characteristics. These insights are due to the nature of the wavelet transform that would not be immediately evident using a traditional Fourier transform approach.

§1. Introduction

Ever since Willard J. Pierson [18] adopted the works of John W. Tukey [22] and introduced the power spectrum analysis to ocean wave studies, Fourier spectrum analysis has been successfully and persistently used in data analysis of wind-generated ocean waves. Over the past four decades, with the increased availability of new instruments for measuring wind and waves, spectrum analysis has continued to be the fundamental standard procedure used for analyzing wind and wave data.

Fourier spectrum analysis generally provides frequency information about the energy content of measured, and presumed stationary, time-series data. Characteristic properties of waves such as total energy and dominant or average frequency can be readily derived from the estimated spectrum. This information, however, pertains only to the time span of the measured data. Changes and variations within a time series cannot be easily unraveled. As stationarity in the data simply represents a mathematical idealization, its validity is usually regarded as an approximation of the real wave field. The effectiveness of applying Fourier spectrum analysis to a rapidly changing wave field, such as during wave growth or decay, is

Wavelets in Geophysics
Efi Foufoula-Georgiou and Praveen Kumar (eds.), pp. 151–166.
ISBN 0-12-262850-0
1994

uncertain. The emergence of wavelet transform analysis which can yield localized time-frequency information without requiring that the time-series be stationary has presented a rewarding and complementary approach to the traditional Fourier spectrum analysis and has advanced significant new perspectives for improved wave data analysis.

While wavelet analysis has been widely recognized as a revolutionary approach applicable to many fields of studies, the application of wavelet transform to wind wave data analysis is still in its infancy. This article mainly presents the author's own attempt at understanding wind-generated waves using the wavelet decomposition.

§2. Wavelet Spectrum

Following a standard formulation [3], we briefly summarize the wavelet transform. We start with a family of functions, the so-called analyzing wavelets, $\psi_{ab}(t)$, that are generated by dilations a and translations b from a mother wavelet, $\psi(t)$, as

$$\psi_{ab}(t) = \frac{1}{\sqrt{|a|}}\psi(\frac{t-b}{a}) \tag{1}$$

where $a > 0$, $-\infty < b < +\infty$, and $\int_{-\infty}^{+\infty}\psi(t)dt = 0$. The continuous wavelet transform of a time-series, $X(t)$, is then defined as the inner product of ψ_{ab} and X as

$$\tilde{X}(a,b) = < \psi_{ab}, X > = \frac{1}{\sqrt{|a|}}\int_{-\infty}^{+\infty} X(t)\psi^*(\frac{t-b}{a})dt \tag{2}$$

or equivalently in terms of their corresponding Fourier transforms

$$\tilde{X}(a,b) = \sqrt{|a|}\int_{-\infty}^{+\infty}\hat{X}(\omega)\hat{\psi}^*(a\omega)e^{ib\omega}d\omega \tag{3}$$

where an asterisk superscript indicates the complex conjugate. In essence the wavelet transform takes a one-dimensional function of time into a two-dimensional function of time and scale (or equivalently, frequency).

In practical applications, the wavelets can be conveniently discretized by setting $a = 2^s$ and $b = \tau 2^s$ in octaves [4] to obtain

$$\psi_{s\tau}(t) = 2^{-s/2}\psi(2^{-s}t - \tau), \tag{4}$$

where s and τ are integers. Then the continuous wavelet transforms (2) and (3) for time series data $X(t)$ become

$$\tilde{X}(s,\tau) = \frac{1}{\sqrt{2^s}}\int_{-\infty}^{+\infty} X(t)\psi^*(\frac{t}{2^s} - \tau)dt \tag{5}$$

and

$$\tilde{X}(s,\tau) = 2^{s/2} \int_{-\infty}^{+\infty} \hat{X}(2^s\omega)\hat{\psi}^*(\omega)e^{i\tau 2^s\omega}d\omega. \tag{6}$$

In general, the studies of wavelet transforms and wavelet analysis are centered on two basic questions [4]: (1) Do the wavelet coefficients completely characterize the time-series data? (2) Can the original time series be reconstructed from the wavelet coefficients? The answers to both of these questions are clearly yes as evidenced by the voluminous literature in recent years. In this paper we rely on the affirmative answer to the first question and concentrate on exploring the wavelet transform of measured wind waves. It is an exciting and fruitful area for practical application of the wavelet transform . As data analysis on wind wave studies comprises mainly of applications of statistics and Fourier transforms, the summary shown in Table 1 indicates that wavelet transform analysis is a logical extension to the currently available analyses.

In analogy with Fourier energy density spectrum, we can readily define a *wavelet spectrum* for a data series $X(t)$ as

$$W_X(s,\tau) = \tilde{X}(s,\tau)\tilde{X}^*(s,\tau) = |\tilde{X}(s,\tau)|^2. \tag{7}$$

There are other designations in the literature for $W_X(s,\tau)$ [21]. Results from the application of short-time Fourier transforms have been called spectrograms, whereas results from the application of wavelet transforms have been called scalograms. Since in practice the scale, s, and translation, τ, can be associated with a corresponding frequency, ω, and time, t, (7) can be considered as a representation of the time-varying, localized energy spectrum for a given time series.

We can similarly define a *cross wavelet spectrum* for the study of two simultaneously measured data sets $X(t)$ and $Y(t)$ as

$$W_{XY}(s,\tau) = \tilde{X}(s,\tau)\tilde{Y}^*(s,\tau) \tag{8}$$

and accordingly,

$$\Gamma(s,\tau) = \frac{W_{XY}(s,\tau)}{\sqrt{W_{X_k}(s,\tau)W_{Y_k}(s,\tau)}} \tag{9}$$

and

$$\Gamma^2(s,\tau) = \frac{[\Re W_{XY}(s,\tau)]^2 + [\Im W_{XY}(s,\tau)]^2}{W_{X_k}(s,\tau)W_{Y_k}(s,\tau)} \tag{10}$$

as the complex-valued wavelet coherency and its square, the real valued wavelet coherence, respectively, between the two data sets. The functions $\Re W_{XY}(s,\tau)$ and $\Im W_{XY}(s,\tau)$ in (10) are respectively the real and imaginary parts of $W_{XY}(s,\tau)$, and hence the co- and quadrature- wavelet spectra of $X(t)$ and $Y(t)$.

Table 1. Analogy of statistics, Fourier transform and wavelet transform analysis.

Statistics	Fourier Transform	Wavelet Transform
Variance	Frequency Spectrum	Wavelet Spectrum
$E(X^2)$	$S_X(\omega) = \hat{X}\hat{X}^* = \lvert\hat{X}\rvert^2$	$W_X(s,\tau) = \tilde{X}\tilde{X}^* = \lvert\tilde{X}\rvert^2$
Covariance	Cross Spectrum	Cross Wavelet Spectrum
$E(XY)$	$S_{XY}(\omega) = \hat{X}\hat{Y}^*$	$W_{XY}(s,\tau) = \tilde{X}\tilde{Y}^*$
Coefficient of Correlation	Coherency	Wavelet Coherency
$r = \frac{E(XY)}{\sqrt{E(X)E(Y)}}$	$\gamma = \frac{S_{XY}(\omega)}{\sqrt{S_X(\omega)S_Y(\omega)}}$	$\Gamma = \frac{W_{XY}(s,\tau)}{\sqrt{W_X(s,\tau)W_Y(s,\tau)}}$
Coefficient of Determination	Coherence	Wavelet Coherence
$r^2 = \frac{[E(XY)]^2}{E(X)E(Y)}$	$\gamma^2 = \frac{\lvert S_{XY}(\omega)\rvert^2}{S_X(\omega)S_Y(\omega)}$	$\Gamma^2 = \frac{\lvert W_{XY}(s,\tau)\rvert^2}{W_X(s,\tau)W_Y(s,\tau)}$

In implementing the applications, there are a number of well-defined continuous wavelet forms available [6]. In this study we choose to use the complex-valued, modulated Gaussian analyzing wavelet known as the Morlet wavelet. This wavelet, originally proposed by Morlet *et al.* [16], ushered in the present wavelet era and is given by

$$\psi(t) = e^{imt}e^{-t^2/2}. \tag{11}$$

Its Fourier transform is

$$\hat{\psi}(\omega) = \sqrt{2\pi}e^{-(\omega-m)^2/2}. \tag{12}$$

Here we should point out that this wavelet is not an admissible wavelet since a correction term is needed because $\hat{\psi}(0) \neq 0$. However, in practice choice of a large enough value for the parameter m, (*e.g.* $m > 5$) generally renders the correction term negligible. In this study, we follow Daubechies [5] and use $m = \pi\sqrt{2/ln2}$. While there are admissible wavelets available, the Morlet wavelet has been widely used in signal analysis and sound pattern studies. Aside from its convenient formulation and historical significance, its localized frequency is independent of time, a feature of particular advantage for wind wave studies.

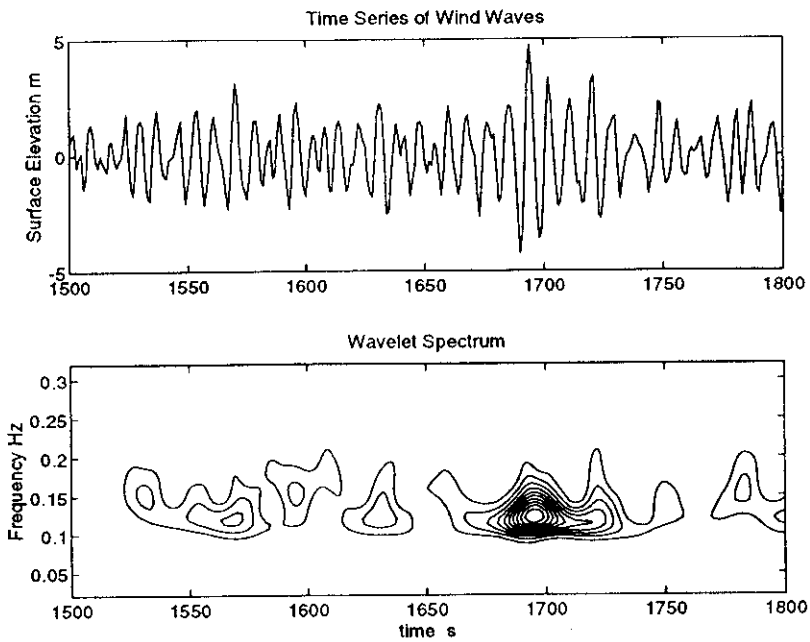

Figure 1. A sample plot of a time series of wind waves and its respective wavelet spectrum.

§3. Applications

In the following three subsections we present three wavelet transform analyses of wind wave data leading to distinct results that would be difficult, if not impossible, to obtain from the usual Fourier transform. The data used in the applications were measured during the recent SWADE (Surface Wave Dynamics Experiment) program [25]. The wind and wave data were recorded from a 3 m discus buoy during the severe storm of October 26, 1990. The buoy was located at latitude 38°22.1′ N and longitude 73°38.9′ W, with a water depth of 115 m near the edge of the continental

shelf offshore of Virginia in the Atlantic Ocean. Time series of wind and waves were both recorded at 1 Hz from a combined design of a three-axis accelerometer and magnetometer along with the Datawell Hippy system. A total of 100 sets of data, each 1024 s in length, were used in the analyses. The data, predominantly wind-generated waves, covered the entire duration of the storm with wind speeds ranging from calm to 18 m/s and significant wave heights approaching 7 m.

3.1. Wave grouping effects

Wind waves appear in groups; i.e., higher waves occur successively in separated sequences. This phenomenon is well-known to seasoned sailors and can sometimes be seen in wind wave recordings. Apart from being a confirmed natural phenomenon, the existence of wave groups tends to challenge the conventional notion that wave data can be considered as a stationary process.

Wave data analysis, aimed at studying wave group characteristics, has been confined to identifying individual groups by counting the number of wave heights that exceed a prescribed height. A group is simply measured by a group length which is the number of waves counted. While statistics of the group lengths can be assessed, efforts have been generally directed at correlating the mean group length with spectral properties of the data [14].

In a wavelet transform analysis of wave data, an examination of a contour plot of resulting wavelet spectrum of waves shows distinct energy density parcels in the time-frequency domain. Figure 1 presents a simultaneous plot of sea surface elevations and the contours of their corresponding wavelet spectrum. The contour patches shown in the figure clearly indicate wave groupings that are visibly identifiable in the time series. The boundary of a wave group can be readily specified by setting an appropriate threshold energy level in the wavelet spectrum. Essentially there is a localized time-frequency energy spectrum for each group of waves, which is potentially more informative than previous approaches.

Based on the boundary specified for each wave group from the wavelet spectrum, we have at least four relevant group parameters to characterize a wave group:

(i) The group time length, t_g, which is the difference between the maximum and minimum time scales the group boundary covered.

(ii) The total group energy, E_g, which is an integration of the local wavelet spectrum over the time length t_g.

(iii) The dominant group frequency, f_p, which is the frequency of the peak energy over the time length t_g.

(iv) The dominant group wave height, h_p, which can be obtained from the time series as the maximum trough-to-crest wave height over the time length t_g.

The variability of these parameters indicates that wave groups are apparently diverse, irregular, nonperiodic, and independent from each other. The formidable task is to determine the significance and usefulness of these parameters. Here we consider a simplified approach of forming two normalized parameters:

- normalized group time length $= t_g * f_p$, and
- normalized total group energy $= E_g/h_p^2$.

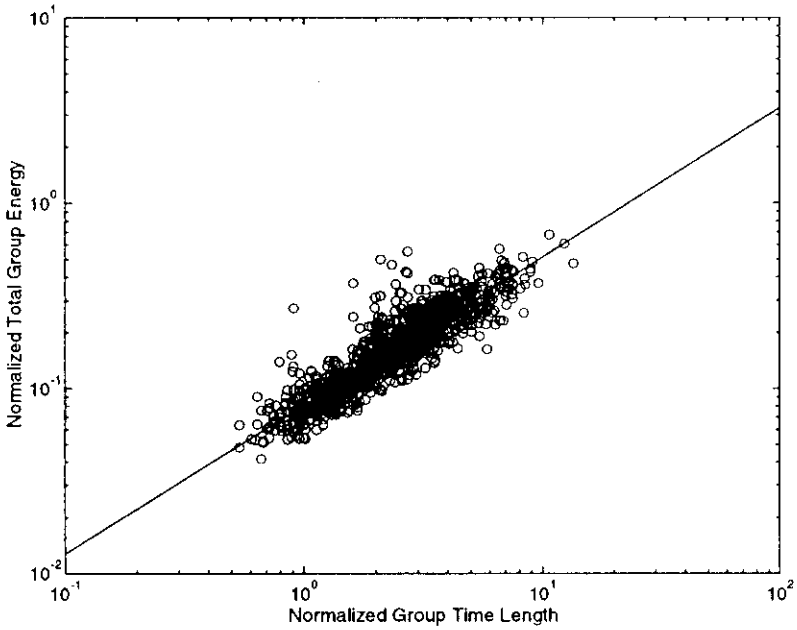

Figure 2. A scatter plot of normalized total group energy versus normalized group time length, the solid line is a linear least square fit for the data.

A scatter plot of these two normalized parameters, shown in Figure 2, indicates a fairly well-defined linear relationship. As the normalized total group energy is a measure of energy content, and the normalized group time length is a measure of the number of waves with possibly the same peak energy frequency, Figure 2 implies, that higher energy content in a

wave group tends to generate more waves in the group. This interesting result, while intuitively understandable, is new.

A scatter plot of averages of dominant group wave heights versus significant wave heights is shown in Figure 3. The significant wave height, defined as the average of the highest one-third wave heights in the wave record, is a familiar and widely-used parameter. For practical applications, such as in engineering design, mean dominant group wave height would be more pertinent than the significant wave height. Figure 3 shows that significant wave heights are slightly less than the averages of dominant group wave heights.

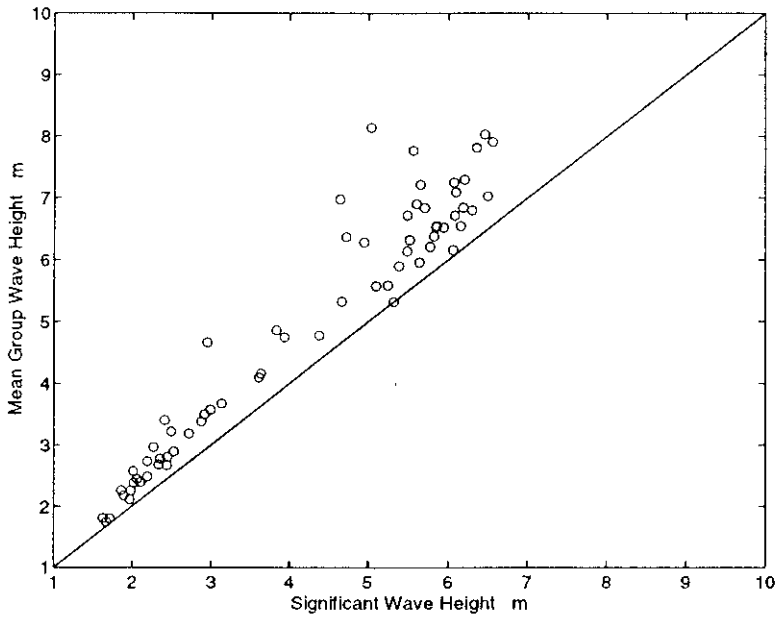

Figure 3. A scatter plot of mean group wave height versus significant-wave height.

3.2. How do wind waves grow?

The wind and waves measurements in the SWADE program introduced a new data collection practice, namely, that wind and waves were measured at the same resolution simultaneously. Previously, wind data were merely collected as hourly averages. The availability of simultaneous high-resolution wind and wave data has provided an unparalleled opportunity to directly examine detailed wind action on waves, especially during wave

growth.

How do wind waves grow? It is a question that several generations of scientists have addressed. In addition to the early work of Jeffreys [11] and Ursell's [23] famous "nothing very satisfying" summary, modern conceptual perceptions of wind waves primarily stem from the theoretical conjectures of Phillips [17], Miles [15], and Hasselmann [8]. The current proliferation of numerical wave models is basically developed from these early theories. Numerous measurements of wave energy spectra with average wind speeds have been conducted for the validation and possible enhancement of the available models. Now with the latest SWADE measurements and the advancement of wavelet transforms, we are able to examine wind wave processes from new perspectives.

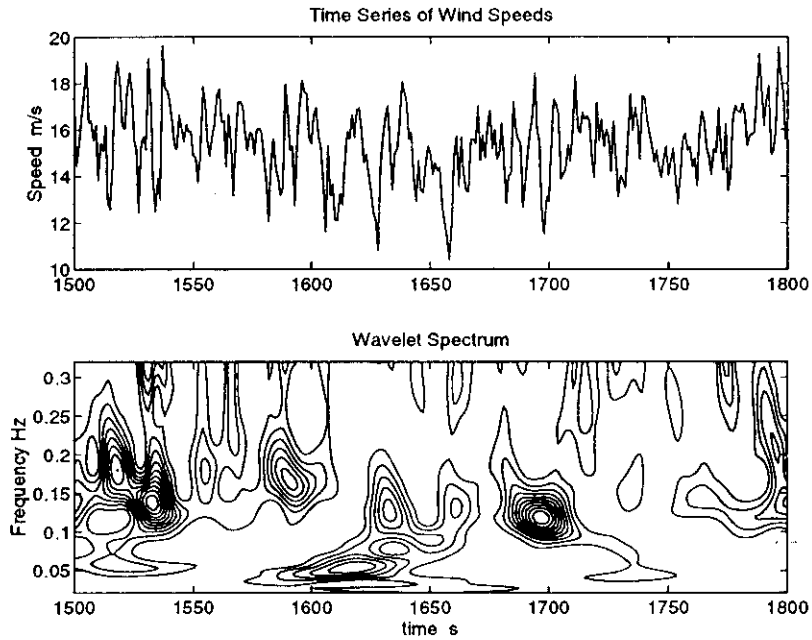

Figure 4. The time series of wind speeds corresponding to the wave data of Figure 1 and its respective wavelet spectrum.

One way of analyzing simultaneously recorded wind and wave measurements is through cross wavelet spectrum analysis. Figure 4 shows a part of the wind speeds and their wavelet spectrum corresponding to the wave data of Figure 1. There is no obvious relationship between the two time series that we can deduce from the top parts of Figures 1 and 4. However, if we consider the wavelet spectrum, a tract of high energy density contours

appears in both spectra over the same frequency ranges and during the time when highest wave heights occurred in the wave time series. Qualitatively we might infer that wind and waves interact immediately during wave growth.

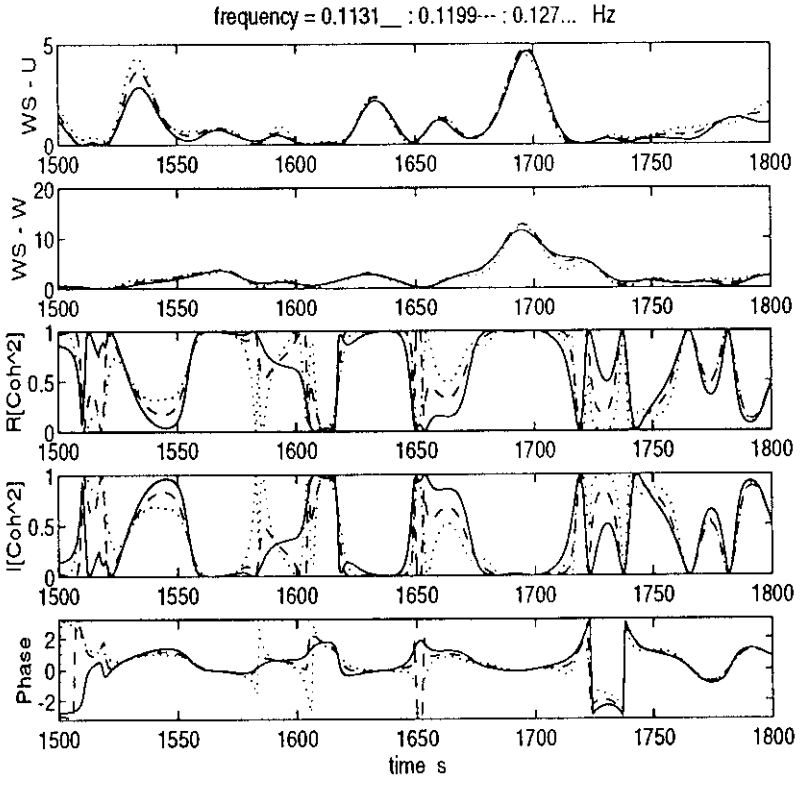

Figure 5. Plots of three peak-energy frequency components versus time. The five subgraphs from top down are, respectively, wavelet spectrum for wind speeds, wavelet spectrum for waves, the real part, the imaginary, and the phase of coherence.

To see if we can verify this inference quantitatively, we calculate the cross wavelet spectrum and their corresponding wavelet coherence for the simultaneous wind and wave data. The results, expressed either in contour or three-dimensional plots, are rather intricate and perplexing. It is not at all clear what we can meanfully deduce. If, however, we plot the results for individual frequencies, we can see some interesting results. Figure 5, corresponding to the same data of Figures 1 and 4, is an example of what these

plots can tell us. The five separate graphs in Figure 5 display, respectively from top down, the wavelet spectrum for wind, the wavelet spectrum for waves, the real part, the imaginary part, and the phase of wavelet coherence. All of the plots contain the three frequency components of 0.1131, 0.1199, and 0.127 Hz for which the energy density is highest.

Note that in Figure 1 there are five groups of waves that can be identified from the wavelet spectrum. In the second graph of Figure 5 in which energy densities increase and decrease with respect to time, only three stronger groups (i.e., at time marks 1570, 1630, and 1695) are reflected from the fluctations of these frequency components. The top graph of Figure 5 shows that the wavelet spectrum components for wind speeds exhibit similar, but more, energy fluctations with time. Some of the fluctuations correspond closely to those of the waves. By examining the bottom three graphs of Figure 5, it shows quite clearly that for the three wave groups identified with appreciable energy contents, the real part of their coherence is close to[1] 1, their imaginary part close to 0, and their phase is also close to 0. Therefore, during wave growth, the frequency components for peak wave energy between wind and waves are inherently *in phase*. Wave groups constitute the basic elements of wind wave processes, and the wave growth are primarily taking place within the wave group.

As the growth of wind waves is an extremely complicated process, the above results contribute still qualitatively toward an understanding of the nature of how do waves grow. While we are accustomed to correlate wave growth with "average" wind speeds, the results presented here clearly show that waves are in fact responding to wind speeds instantly. Further detailed studies may challenge or counter more familiar notions of wind waves. Using cross wavelet spectrum analysis not only introduces new data analysis techniques, it may also leads to new courses of exploration.

3.3. Detecting breaking waves

Wave breaking is a familiar phenomenon that occurs intermittently and ubiquitously on the ocean surface. It is visible from the appearance of the whitecaps, yet it can not be readily measured with customary instruments. Wave breaking has been recognized as playing a crucial role in accurate estimations of the exchange of gases between the ocean and the atmosphere [24] and in the transfer of momentum from wind to the ocean surface [1]. Most of the practical works on wave breaking [2], both

[1] Unlike the Fourier cross spectrum analysis where averaging can be used to avoid coherence being identically one, we have to use the real and imaginary parts of the coherence separately here, since their sum, the coherence, is indeed identically one in this formulation. On the other hand, this approach successfully substantiates the use of the co- and quadrature spectra [19] to signify their "in phase" and "out of phase" properties, respectively.

in the laboratory and in the field, have been done with specialized methods based on radar reflectivity, optical contrast, or acoustic output of the ocean surface. Here we show that with the help of wavelet spectra [12], instead of using specialized measurement devices, a basic wave-breaking criterion can be easily implemented to wind wave time series to distinguish breaking from non-breaking waves. This simple and fairly efficient approach can be readily applied to indirectly estimate wave breaking statistics from any available time series of wind-generated waves.

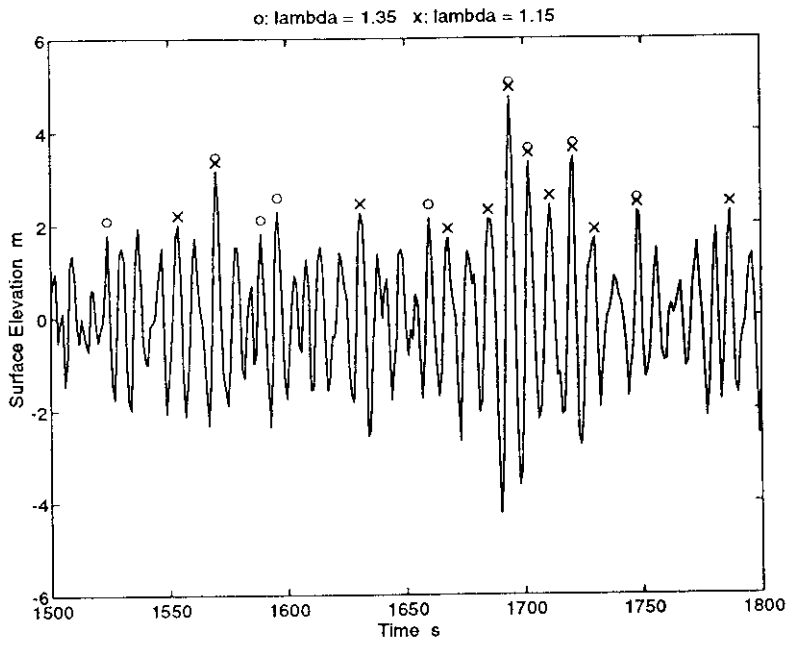

Figure 6. A sample plot of a time series of wind waves, same as Figure 1, with possible breaking waves marked by o's and x's indicating different high frequency ranges $\lambda\omega_p : \omega_n$ defined by the λ values given at the top of the figure.

One of the most frequently used approaches for the study of wave breaking is the use of a limiting value of the wave steepness beyond which the surface cannot be sustained [13]. Alternatively, assuming a linear dispersion relationship, the wave surface will break when its downward acceleration exceeds a limiting fraction, γ, of the gravitational acceleration, g, that is $a\sigma^2 \cong \gamma g$. The quantity $a\sigma^2$ can be calculated for a time series of wave data since the local wave amplitude, a, is available from the measured time-series while the local wave frequency, σ, can be obtained from the wavelet

spectrum. In classical studies, it has generally been assumed that $\gamma = 0.5$. Recent laboratory studies [10] have shown that γ is closer to 0.4. Some field measurements [9] further indicate that the value of γ should even be lower. In this study we chose to follow the laboratory results and use $\gamma = 0.4$.

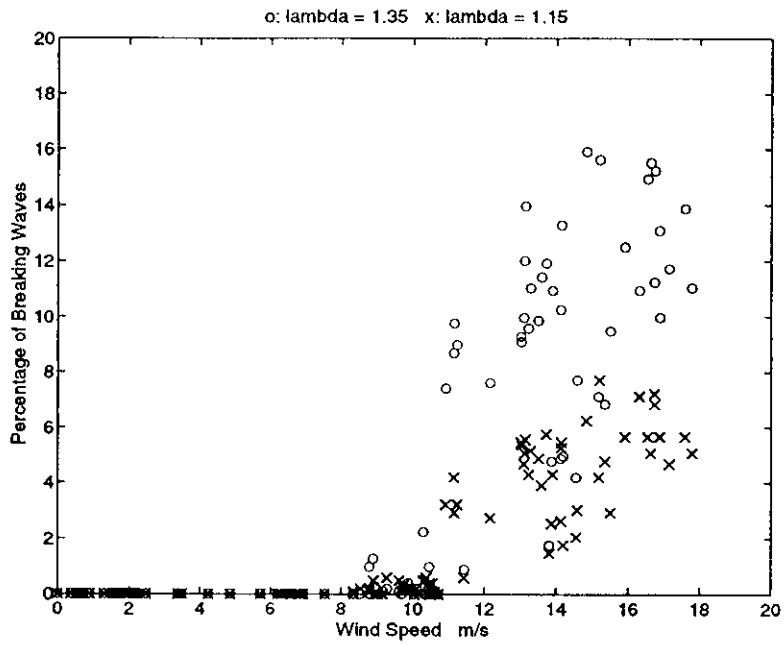

Figure 7. Plot of the percentage of breaking waves with respect to wind speeds. The o's and x's are the same as defined in Figure 6.

Since the wavelet transform provides an equivalent time-frequency spectrum, $W_X(\omega, t)$, for the wind wave time series, then there is a localized frequency spectrum at each data point, $X(t_i)$, given by

$$\Phi_i(\omega) = [W_X(\omega, t)]_{t=t_i}.$$

It is not immediately clear which frequency should be used for σ in calculating $a\sigma^2$. Because breaking events are generally associated with the high frequency part of the spectrum, for each $X(t_i)$ we chose to define a σ_i as the average frequency [20] over the high frequency range, $\lambda\omega_p : \omega_n$, of the localized spectrum at $t = t_i$ as

$$\sigma_i = \left[\frac{\int_{\lambda\omega_p}^{\omega_n} \omega^2 \Phi_i(\omega) d\omega}{\int_{\lambda\omega_p}^{\omega_n} \Phi_i(\omega) d\omega} \right]^{1/2}$$

where ω_p is the localized frequency at the energy peak, ω_n is the cut-off

frequency, and λ is a number greater than 1 that denotes the start of the high frequency range beyond ω_p. The exact location of this high frequency range has not been clearly defined. Considering this range as corresponding to the familiar equilibrium range, one frequently used value of λ has been 1.35 [7].

To test this approach, Figure 6 presents an illustration of the analysis where estimated breaking waves are marked on the same time series segment given in figure 1. The x's and o's represent the results with a high frequency range between 1.15 and 1.35 times, respectively, of the local peak energy frequency, ω_p, and cut-off frequency, ω_n. While the λ values of 1.15 or 1.35 has been chosen rather arbitrarily for comparisons, they are clearly not always recognizing the same breaking waves. In general with the same cut-off frequency, the lower end of the frequency range farther away from the local peak frequency, i.e. large λ value, would yield higher local average frequency σ and more breaking waves. Therefore an exploration of breaking waves could potentially serve to resolve the definition of the well-known but still not yet well-defined equilibrium range. Figures 7 present plots of overall percentages of breaking waves from all the data analyzed in this study as a function of wind speed. While the data points are scattered considerably, there is an approximate linear trend indicating an increase in the percentage of breaking waves with an increase in wind speed. The results shown in Figure 7 are in general accord with various available observations [9]. According to these results, breaking waves become prevalent when wind speeds exceed 10 m/s.

At the present, the limiting fraction of downward wave acceleration from the gravitational acceleration, γ, and the parameter locating the local equilibrium range beyond local peak frequency, λ, are both tentative. Therefore, the wavelet transform approach that leads to these results is useful, convenient, and also exploratory. Perhaps a better simultaneous measurement of wind-wave time series and wave breaking would suffice to substantiate the approach. Unfortunately operational and sufficient instrument for this simple purpose is still lacking.

§4. Concluding Remarks

We anticipate two groups of readers who might be benefit from this paper, namely, those interested in wavelet applications and those interested in wind wave studies. As this is a first attempt in applying the wavelet transform to wind waves, the results are inevitably primitive. We hope we have succeeded at least in demonstrating the rich potentials for wavelet analysis. There are many important analysis issues that must yet be addressed, including rigorous basis for the cross wavelet spectrum analysis which we have used here. For the wind wave studies, wavelets certainly

provide ample opportunities for data analysis. From the encouraging results we reported here, we are justified in being optimistic.

References

1. Agrawal, Y. C., E. A. Terray, M. A. Donelan, P. A. Hwang, A. J. Williams III, W. M. Drennan, K. K. Kahma, and S. A. Kitaigorodiski, Enhanced dissipation of kinetic energy beneath surface waves, *Nature*, **359**, 219–220, 1992.
2. Banner, M. L., and D. H. Peregrine, Wave breaking in deep water, *Annu. Rev. Fluid Mech.*, **25**, 373–397, 1993.
3. Combes, J. A., A. Grossmann, and Ph. Tchamitchian (Eds.), *Wavelets, Time-Frequency Methods and Phase Space*, 2nd ed. Springer-Verlag, 1989.
4. Daubechies, I., *Ten Lectures on Wavelets*, Society of Industrial and Applied Mathematics, 1992.
5. Daubechies, I., The wavelet transform, time-frequency localization and signal analysis, *IEEE Trans. Inform. Theory*, **36**, 961–1005, 1990.
6. Farge, M., Wavelet transforms and their applications to turbulence, *Annu. Rev. Fluid Mech.*, **24**, 395–457, 1992.
7. Gunther, H., W. Rosenthal, T. J. Weare, B. A. Worthington, K. Hasselmann, and J. A. Ewing, A hybrid parametrical wave prediction model, *J. Geophys. Res.*, **84**, 5727–5738, 1979.
8. Hasselmann, K., On the non-linear energy transfer in a gravity-wave spectrum, Part 1, General theory, *J. Fluid Mech.*, **12**, 481–500, 1962.
9. Holthuijsen, L. H., and T. H. C. Herbers, Statistics of breaking waves observed as whitecaps in the open sea, *J. Phys. Oceanogr.*, **16**, 290–297, 1986.
10. Hwang, P. A., D. Xu, and J. Wu, Breaking of wind-generated waves: measurements and characteristics, *J. Fluid Mech.*, **202**, 177–200, 1989.
11. Jeffreys, H., On the formation of water waves by wind, *Proc. Roy. Soc.*, bf A 107, 189–206, 1925.
12. Liu, P. C., Estimating breaking wave statistics from wind-wave time series data, *Annales Geophysicae*, **4**, 970–972, 1993.
13. Longuet-Higgins, M. S., On wave breaking and the equilibrium spectrum of wind -generating waves, *Proc. Roy. Soc.*, **A 310**, 151–159, 1969.
14. Masson, D. and P. Chandler, Wave groups, a closer look at spectral methods, *Coastal Engineering*, **20**, 249–275, 1993.
15. Miles, J. W., On the generation of surface waves by shear flows, *J. Fluid Mech.*, **3**, 185–204, 1957.
16. Morlet, J., G. Arens, I. Fourgeau, and D. Giard, Wave propagation and sampling theory, *Geophysics*, **47**, 203–236, 1982.

17. Phillips, O. M., On the generation of waves by turbulent wind, *J. Fluid Mech.*, **2**, 417–455, 1957.
18. Pierson, W. J., and W. Marks, The power spectrum analysis of ocean wave record, *Trans. Amer. Geophys. Un.*, **33**, 834–844, 1952.
19. Priestley, M. B., *Spectral Analysis and Time Series*, Academic Press, 1981.
20. Rice, S. O., Mathematical analysis of random noise, in *Noise and Stochastic Processes* (N. Wax, ed.), Dover, New York, 133–294, 1954.
21. Rioul, O., and F. Flandrin, Time-scale energy distribution: a general class extending wavelet transforms, *IEEE Trans. Signal Processing*, **40**, 1746–1757, 1992.
22. Tukey, J. W., The sampling theory of power spectrum estimates, *Symposium on Applications of Autocorrelation Analysis to Physical Problems*, NAVEXOS-0-735, Office of Naval Research, 1949.
23. Ursell, F., Wave generation by wind, in *Surveys in Mechanics*, Cambridge University Press, 216–249, 1956.
24. Wallace, D. W. R., and C. D. Wirick, Large air-sea gas fluxes associated with breaking waves, *Nature*, **356**, 694–696, 1992.
25. Weller, R. A., M. A. Donelan, M. G., Briscoe, and N. E. Huang, Riding the crest: A tale of two wave experiments, *Bulletin Am. Meteorol. Soc.*, **72**, 163–183, 1991.

This is GLERL Contribution no. 873. Partial financial support to initiate this study was provided by the U.S. Office of Naval Research. This study was also benefited from early collaborations with A. K. Liu and B. Chapron.

Paul C. Liu
NOAA Great Lakes Environmental Research Laboratory
Ann Arbor, Michigan
e-mail: *liu@glerl.noaa.gov*
1994